

Article

Numerical Reservoir Simulation of Supercritical Multi-Source and Multi-Component Steam Injection for Offshore Heavy Oil Development

Qiang Fu ¹, Zhouyuan Zhu ^{2,*} , Junjian Li ³, Hongmei Jiao ¹, Shuoliang Wang ⁴, Huiyun Wen ¹ and Yongfei Liu ¹

¹ State Key Laboratory of Natural Gas Hydrates, CNOOC Research Institute Ltd., Beijing 100027, China; fuqiang8@cnooc.com.cn (Q.F.); jiaohm@cnooc.com.cn (H.J.); wenhy@cnooc.com.cn (H.W.); liuyf38@cnooc.com.cn (Y.L.)

² College of Safety and Ocean Engineering, China University of Petroleum (Beijing), Beijing 102249, China

³ School of Petroleum Engineering, China University of Petroleum (Beijing), Beijing 102249, China; junjian@cup.edu.cn

⁴ School of Energy Resources, China University of Geosciences (Beijing), Beijing 100083, China; wangshuoliang@cugb.edu.cn

* Correspondence: zhuzy02@cup.edu.cn

Abstract: We present the workflow for numerical reservoir simulation of supercritical multi-source and multi-component steam injection for offshore heavy oil development. We have developed unique techniques in a commercial reservoir simulator to implement the thermal properties of supercritical multi-source and multi-component steam, the pyrolysis chemical reactions, the temperature-dependent relative permeability, and the process of partially dissolving the sandstone rock to enhance the matrix permeability in a commercial reservoir simulator. Simulations are conducted on the type pattern reservoir model, which represents one of the heavy oil fields in CNOOC's Bohai Bay oil field. Simulation input parameters are calibrated based on laboratory experiments conducted for supercritical multi-source and multi-component steam injection. Simulation results have shown clear improvements in injecting supercritical multi-source and multi-component steam in offshore heavy oil reservoirs compared to the normal steam injection process using subcritical steam. This serves as a workflow for implementing a numerical simulation of the novel supercritical multi-source and multi-component steam injection recovery process.

Keywords: supercritical multi-source and multi-component steam; thermal reservoir simulation; offshore heavy oil development; pyrolysis reaction; mineral dissolution



Citation: Fu, Q.; Zhu, Z.; Li, J.; Jiao, H.; Wang, S.; Wen, H.; Liu, Y. Numerical Reservoir Simulation of Supercritical Multi-Source and Multi-Component Steam Injection for Offshore Heavy Oil Development. *Processes* **2024**, *12*, 216. <https://doi.org/10.3390/pr12010216>

Academic Editors: Qingbang Meng and Yongping Chen

Received: 15 November 2023

Revised: 29 December 2023

Accepted: 11 January 2024

Published: 18 January 2024



Copyright: © 2024 by the authors. Licensee MDPI, Basel, Switzerland. This article is an open access article distributed under the terms and conditions of the Creative Commons Attribution (CC BY) license (<https://creativecommons.org/licenses/by/4.0/>).

1. Introduction

Offshore heavy oil accounts for large resource potential for the future of the world oil supply. For example, in Bohai Bay, China alone, 4 billion barrels of heavy oil have been discovered. Such heavy oil resources are yet expected to be fully developed, potentially using certain Enhanced Oil Recovery (EOR) techniques. Steam-based thermal recovery techniques are the most widely used EOR methods for heavy oil development onshore [1]. The most well-known steam flooding project is the Kern River oilfield in California, which has been steam-flooded since about the 1960s. For example, the heavy oil resources in the Liaohe and Xinjiang oil fields in China are successfully unlocked and developed using cyclic steam stimulation, steam flooding, and steam-assisted gravity drainage techniques. The in situ combustion process, also known as fireflooding, which injects air into the reservoir to combust part of the oil to generate heat and pressure to mobilize the remaining oil, is also implemented in oilfields such as the Suplacu field in Romania. Offshore oil fields, however, have seen rare commercial success in implementing steam-based thermal EOR technologies. Early trials include Elf's cyclic steam stimulation tests in the Emeraue field offshore Congo [2].

To overcome this challenge of offshore thermal heavy oil recovery, the China National Offshore Oil Company (CNOOC) has implemented a series of thermal heavy oil recovery field trials and even started early commercial thermal heavy oil production in Bohai Bay, China, in recent years. The early field pilots have demonstrated great potential for offshore heavy oil thermal recovery by using co-injection of steam and gases in a cyclic steam stimulation mode [3–7]. The basic recovery technique deployed is normal cyclic steam injection with co-injection of gases. A specially designed small-sized steam generator that consumes diesel fuel and co-generates gases such as CO₂ and N₂ is utilized. Based on all these efforts, the Lvda-21-2 offshore heavy oil field in Bohai Bay, China, has now been commercially developed using the cyclic steam stimulation process. 16 horizontal wells using cyclic steam stimulation have been drilled and completed on the platform of Lvda-21-2. On average, one to two cycles of steam injection have already been applied to these wells up to date. Besides the efforts in offshore thermal heavy oil production, the CNOOC has also been an active player in the efficient development of gas hydrates in China [8,9].

During our endeavor of offshore thermal heavy oil recovery, the CNOOC has focused on a new technology called supercritical multi-source and multi-component steam injection. Supercritical multi-source and multi-component steam injection shows great improvements over normal steam injection using subcritical steam, especially for offshore heavy oil development [10]. A novel designed supercritical multi-source and multi-component steam generator specially suits the small space on offshore platforms designed by the CNOOC. The new steam generator shows great improvements over the previous version of the steam generator in reducing the high energy consumption and cutting off the strong dependence on diesel fuel. The supercritical multi-source, multi-component thermal fluid generator can utilize multi-source fuel, including oily wastewater and crude oil, to generate a thermal fluid that can be directly injected into the injection well. Such thermal fluid mainly contains supercritical steam and other gases, including CO₂ and N₂. This novel steam generator effectively solves the problem of how to obtain fuel locally for offshore heavy oil thermal recovery, reducing the processing cost of oily wastewater on offshore platforms, and is particularly suitable for offshore heavy oil development. Supercritical multi-source and multi-component steam injection into the heavy oil reservoir is well known for its capability to invoke certain recovery mechanisms inside the reservoir, including supercritical steam dissolving the crude oil at any mixing ratio, cracking the heavy oil molecules into smaller oil molecules with the high-temperature pyrolysis reactions, inducing temperature-dependent relative permeability effects which leads the rock to be more water wet at high temperature [11], and also the partial dissolving of the sandstone rock to enhance the matrix permeability at high temperature. All these mechanisms contribute to improved oil recovery than normal steam injection.

Implementing numerical reservoir simulation of supercritical multi-source and multi-component steam injection process, however, is a challenging task, especially the special treatment of these novel recovery mechanisms. In this work, we have implemented the thermal properties of supercritical multi-source and multi-component steam, the pyrolysis chemical reactions, the temperature-dependent relative permeability, and the process of partially dissolving the sandstone rock to enhance the matrix permeability in a commercial reservoir simulator. We have successfully simulated the complex mechanisms in a supercritical multi-source and multi-component steam injection process. The details are discussed as follows. This should serve as a novel workflow for implementing a numerical simulation of the supercritical multi-source and multi-component steam injection recovery process.

2. Materials and Methods

The commercial reservoir simulator CMG STARS is used in this study to simulate the subcritical and supercritical multi-source and multi-component steam injection process in the Lvda-21-2 heavy oil field [12]. We are able to build a single well-type pattern model

based on the full-field model of the Lvda-21-2 oil field of Bohai Bay. The basic reservoir properties are listed in Table 1.

Table 1. Single well type pattern model basic reservoir properties.

Model Settings	Parameter Name	Value	Parameter Name	Value
Grid and Reservoir	Reservoir Model Size (m)	$153 \times 400 \times 30$	Rock Thermal Conductivity (J/m·day·°C)	2.7×10^5
	Reservoir Depth (m)	1500	Rock Heat Capacity (J/m ³ ·°C)	2.3×10^6
	Average Reservoir Permeability (mD)	2500	Average Reservoir Porosity	0.3
	Overburden/Underburden Heat Capacity (J/m ³ ·°C)	2.3×10^6	Overburden/Underburden Thermal conductivity(J/m·day·°C)	1.5×10^5
Oil Properties	Live Oil Density (g/cm ³)	0.964	Dead Oil Density (g/cm ³)	0.984
	Gas Oil Ratio (m ³ /m ³)	4.3	Live Oil Bubble Point (MPa)	1.3
Initial Reservoir Conditions	Initial Reservoir Pressure (MPa)	15.3	Initial Reservoir Temperature (°C)	54
	Initial Oil Saturation	0.55	Initial Water Saturation	0.45
Well Configurations	Wellbore Radius (cm)	7.62	Well Horizontal Length (m)	300

We have inherited the normal default input parameters for subcritical and supercritical steam from CMG STARS in this study. The default steam table in the commercial reservoir simulator is used in this study.

For crude oil, we have defined a dead oil component and a solution gas component to represent the live oil. The fluid properties are listed in Table 2. We adjust component property parameters such as the K-value of different components so that we match the PVT of the live oil, including formation volume factor, live oil gas oil ratio, live oil viscosity, etc. Figure 1 further shows the temperature-viscosity curve for the crude oil from the Lvda-21-2 oil field. As the temperature increases, the in-situ viscosity drops from thousands of cp to a few cp, which is typical for heavy oil.

Table 2. Fluid properties.

Component Name	Dead Oil	Solution Gas
Molar Mass (g/mol)	166	16.3
Critical Pressure P_c (kPa)	1472	4573.81
Critical Temperature T_c (°C)	1168	−84.15
K-value Coefficient KV1	0	1.033×10^6
K-value Coefficient KV4	0	−1024.3
K-value Coefficient KV5	0	−273.15
Initial Mole Fractions in Oil Phase	0.97	0.03
Heat Capacity Coefficient CPG1 (J/gmol·C)	332	19.031
Heat Capacity Coefficient CPG2 (J/gmol·C)	0	5.559×10^{-2}
Mass Density (kg/m ³)	985	123
Compressibility (1/kPa)	1×10^{-6}	1×10^{-6}
Thermal Expansion Coefficient (1/°C)	5×10^{-4}	5×10^{-4}

The relative permeability curves used in this study are shown in Figure 2. As we know, during thermal EOR operations, especially when injecting the relatively high-temperature supercritical multi-source and multi-component steam, the sandstone matrix rock usually tends to be more water-wet at such elevated temperatures [11]. This often leads the water-oil relative permeability curve to shift to the right-hand side, leading to lower residual oil saturation values. We have implemented such temperature-dependent relative permeability endpoints, as shown in Table 3. Such endpoints are matched to our in-house laboratory relative permeability curve measurements at high temperatures.

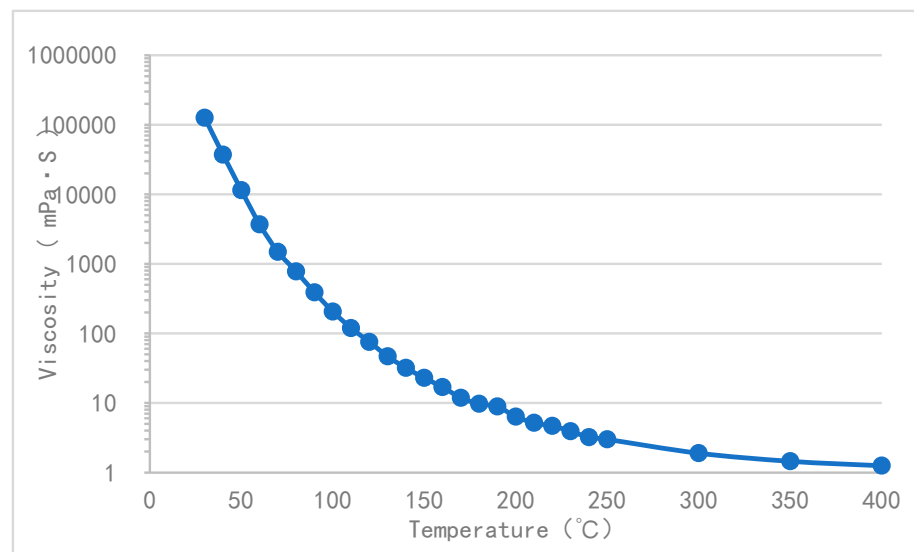


Figure 1. Crude oil temperature-viscosity curve for Lvda-21-2.

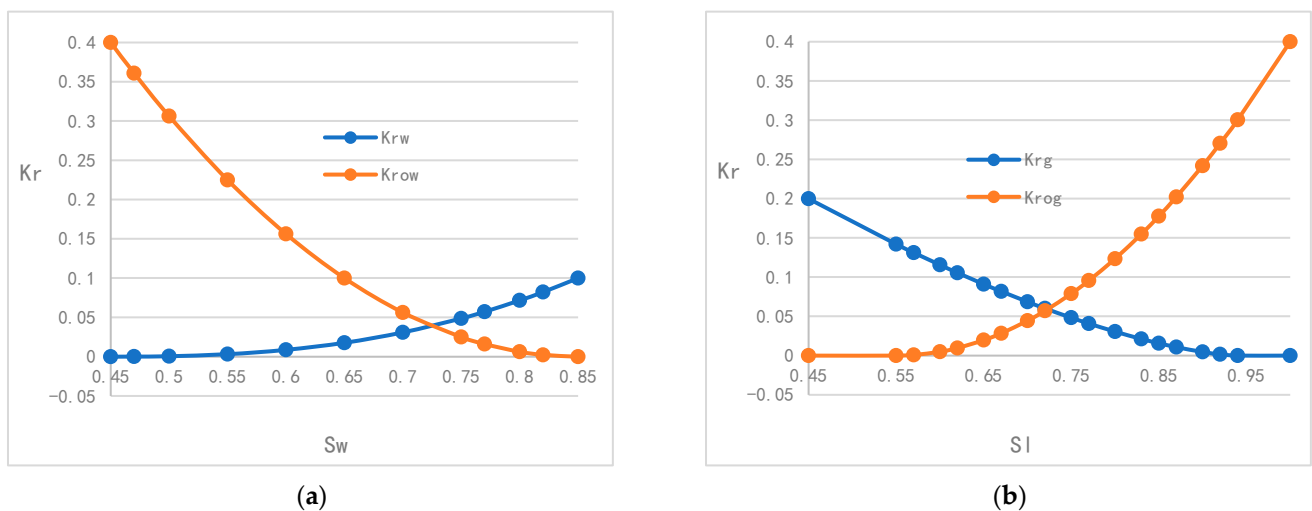
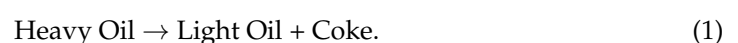


Figure 2. Relative Permeability: (a) Oil-water relative permeability curve; (b) Gas-liquid relative permeability curve.

Table 3. Temperature Dependent Relative Permeability End Points.

Temperature	S_{orw}	K_{rwiro}	S_{wr}
54 °C	0.15	0.10	0.45
150 °C	0.10	0.075	0.50
250 °C	0.05	0.05	0.55
350 °C	0.0	0.025	0.60

Crude oil has well known to have pyrolysis or cracking reactions at the temperature range of more than 300 °C [13]. This pyrolysis kinetic reaction has been studied and numerically simulated in in-situ combustion heavy oil recovery processes [14]. Based on our in-house laboratory experiments, we have implemented a self-defined pyrolysis kinetic reaction in the CMG STARS simulator for the high-temperature supercritical multi-source and multi-component steam injection. A crude oil cracking pseudo-reaction equation based on pseudo components is defined as:



Heavy Oil, Light Oil and Coke are self-defined oil components in CMG STARS. Coke is solid, which is the heavy residue from the pyrolysis reaction at elevated temperatures. Heavy oil and light oil are oleic components, which have higher and lower molecular weight and viscosities, respectively. Under high-temperature conditions of the supercritical multi-source and multi-component steam injection, the Heavy Oil components crack into solid Coke and Light Oil components. The crude oil cracking reaction settings, including reaction order, activation energy pre-exponential factor, etc., are described in Table 4. The kinetic parameters are calibrated to our in-house laboratory reaction kinetics experiments.

Table 4. Heavy oil cracking reaction settings.

Molar Mass (g/mol)	Heavy Oil	675
	Light Oil	157
	Coke	13
Stoichiometric Coefficients for the Crude Oil Pyrolysis Reaction Model	Heavy Oil	−1
	Light Oil	2.154
	Coke	25.96
Heavy Oil Pyrolysis Reaction Model Reaction Kinetics Data	Reaction Order m_γ	1
	Activation Energy E_k^γ (kJ/mol)	62.802
	Pre-exponential Factor α_γ	4.1670×10^5
	Reaction Enthalpy ΔE_γ^r (kJ/mol)	93

Supercritical multi-source and multi-component steam injection process, due to its high temperature, is known to have the capability to partially dissolve the sandstone rock minerals to enhance both the porosity and permeability of the reservoir [10]. Based on laboratory experiments, the mineral dissolution process is also defined for the high-temperature supercritical multi-source and multi-component steam injection. We have defined an initially present solid component inside the reservoir, called Dissolvable Rock, which takes up to 5% of the initial pore space. Using the kinetic chemical reactions in CMG STARS, we defined a rock dissolution process reaction, which only takes place at the elevated temperature of the supercritical multi-source and multi-component steam:



Table 5 shows the rock dissolving kinetic reaction settings, including reaction order, activation energy and pre-exponential factor, etc. Once the solid Dissolvable Rock dissolves, the porosity of the rock matrix increases. Based on the Carmen-Kozeny equation, we further define the effective permeability of the rock as a function of the porosity:

$$K(\varnothing) = K_o \left(\frac{\varnothing}{\varnothing_o} \right)^n \left(\frac{1 - \varnothing_o}{1 - \varnothing} \right)^2. \quad (3)$$

In this way, we model the effective permeability increase due to the dissolution of rock minerals in supercritical multi-source and multi-component steam injection process. A similar numerical simulation approach is also implemented for solid coke deposition-induced permeability reduction effects in the in situ combustion process [15].

Table 5. Dissolvable Rock dissolving reaction settings.

Molar Mass (g/mol)	Dissolvable Rock	13
	Water	18
Stoichiometric Coefficients for the Rock Dissolution Reaction Model	Dissolvable Rock	−1
	Water	0.722
Rock Dissolution Reaction Model Reaction Kinetics Data	Reaction Order m_γ	1
	Activation Energy E_a^γ (kJ/mol)	125
	Pre-exponential Factor α_γ	5×10^9

3. Results

We implement a single well-type pattern model to study the effects of supercritical multi-source and multi-component steam injection in the Lvda-21-2 heavy oil field. The type pattern reservoir model is 400 m long, 150 m wide, and 30 m thick. A horizontal well with a length of 300 m is deployed at the center bottom of the reservoir. This configuration is representative of the production wells in the Lvda-21-2 oil field. A qualitative history match is conducted initially to ensure the type model really represents the actual basic cyclic steam stimulation production process in the Lvda-21-2 oil field. We have conducted primary depletion for 275 days, with a producer's maximum liquid production rate of 80 m³/day and minimum producer bottom-hole pressure of 500 kPa. Then, the well undergoes five cycles of cyclic steam stimulation. Each cycle starts with 25 days of steam injection, which is followed by an immediate production period of 275 days. The producer also produces at the liquid rate of 80 m³/day and a minimum producer bottom-hole pressure of 500 kPa during the production period.

We start with normal subcritical steam injection with a steam temperature of 300 °C, steam injection rate of 220 m³/day (cold water equivalent), and steam quality of 80%. Figure 3 shows the oil production rate, water production rate, and steam injection rate of the basic cyclic steam stimulation process using subcritical steam. As we can see, after the slug of steam injection, a large volume of water and oil is produced back into the producer. We observe an initial high water production rate, which declines continuously. The oil production starts with low values, which increases and then decreases as the reservoir depletes. Figure 4 further shows the producer well bottom-hole pressure and average reservoir pressure of the basic cyclic stimulation process. As more and more cycles of cyclic steaming are applied to the reservoir, the pressure in the reservoir gradually declines. Figure 5 shows the reservoir temperature and oil saturation distribution of the basic cyclic steam stimulation process at the end of the steam injection period of the fifth cycle. Figure 6 further shows the cross-sectional reservoir temperature (left) and oil saturation (right) distribution of the basic cyclic steam stimulation process with subcritical steam at the end of the steam injection period of the fifth cycle. As we can see, a steam chamber is formed above the horizontal producer after five cycles of steam injection. Oil has been produced due to cyclic steam stimulation from the near-well region of the horizontal producer. Figure 7 further shows the cumulative oil production of the basic cyclic steam stimulation process with subcritical steam. The production shown from the reservoir simulation gives pleasant performance for subcritical steam injection.

The supercritical multi-source and multi-component steam injection process is simulated in the next stage. Most of the basic reservoir and fluid settings are kept the same as the subcritical steam injection process. We have, however, shifted to a slug of supercritical multi-source and multi-component steam injection in the cyclic steam stimulation process. We have used the default supercritical steam properties from the commercial reservoir simulator CMG STARS. The injection steam temperature is set to 390 °C, and the injection steam pressure is set to 25 MPa. We also co-inject 10,000 m³/day of standard

condition 40% CO₂ and 60% N₂ together with the steam at the same injection pressure and temperature. Of course, at such high temperatures, the temperature-dependent relative permeability effects will be more profound, causing the rock matrix to be more water-wet than the subcritical steam injection process. At the same time, at such high temperatures, the chemical reaction of pyrolysis reaction will also start to take place, causing an upgrading effect of the crude oil. The rock matrix will also dissolve under the high temperature of supercritical multi-source and multi-component steam, causing the sandstone permeability to be higher.

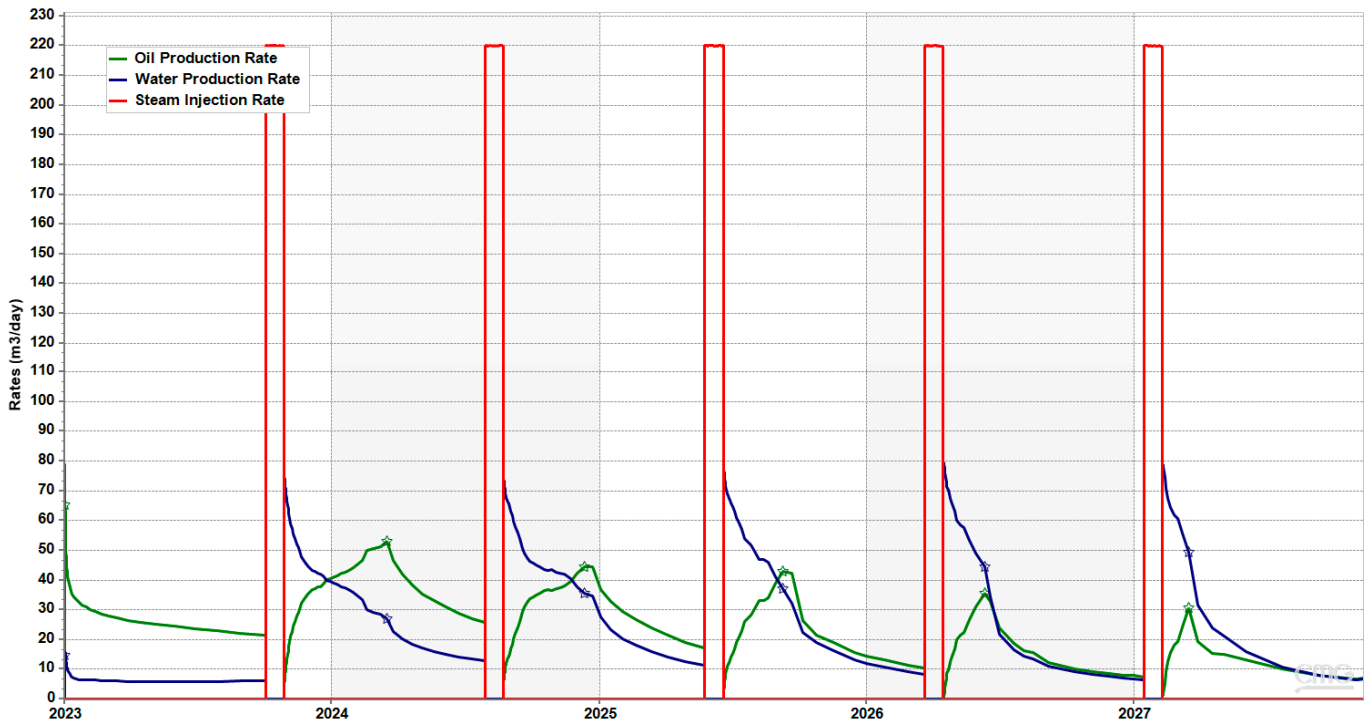


Figure 3. Oil production rate, water production rate, and steam injection rate of the basic cyclic steam stimulation process with subcritical steam.

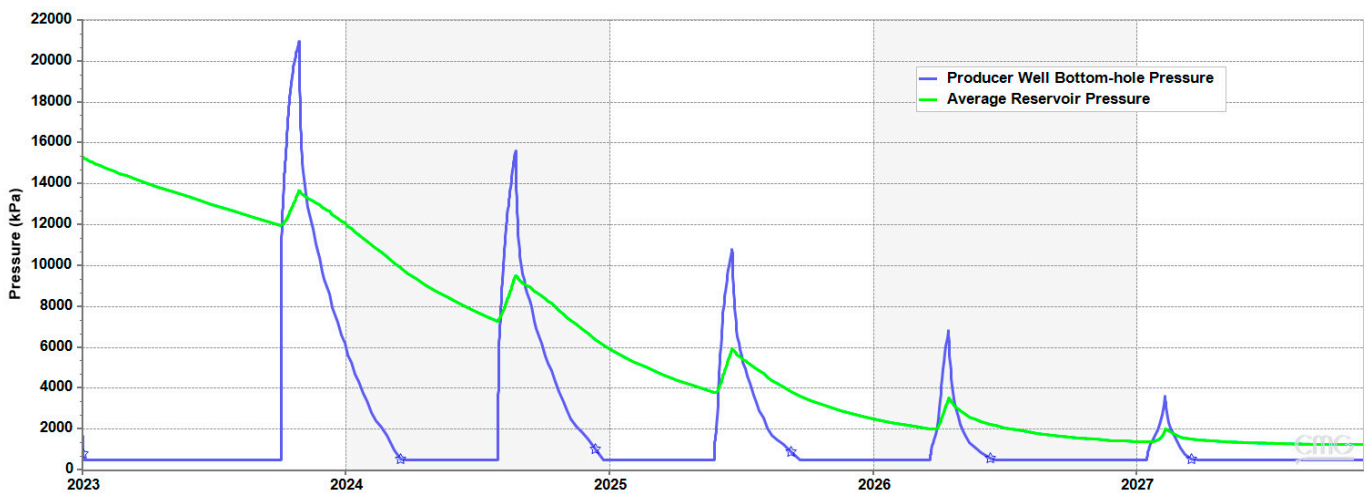


Figure 4. Producer well bottom-hole pressure and average reservoir pressure of the basic cyclic steam stimulation process with subcritical steam.

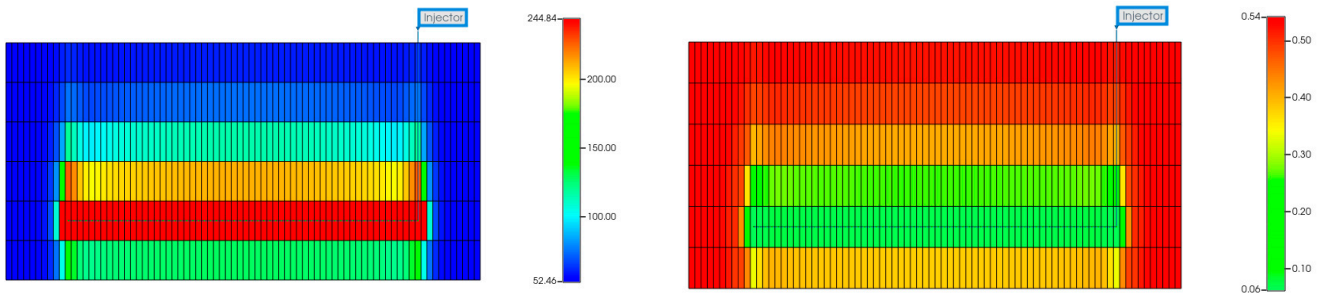


Figure 5. Along the horizontal well, reservoir temperature (left) and oil saturation (right) distribution of the basic cyclic steam stimulation process with subcritical steam at the end of the steam injection period of the fifth cycle.

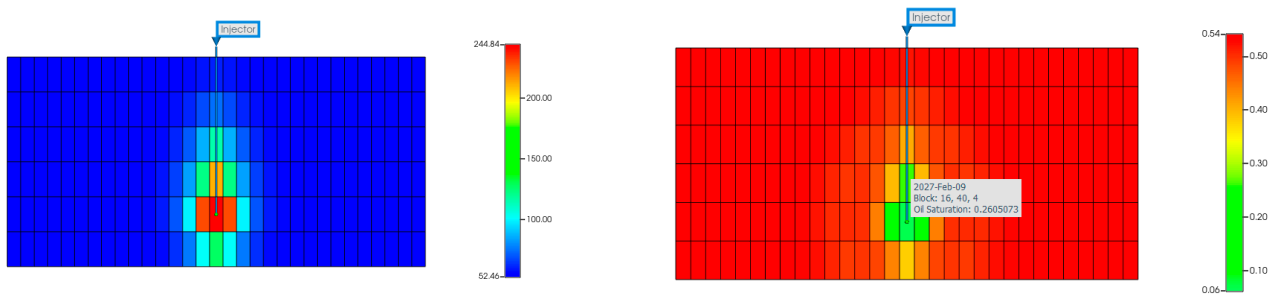


Figure 6. Cross-sectional reservoir temperature (left) and oil saturation (right) distribution of the basic cyclic steam stimulation process with subcritical steam at the end of the steam injection period of the fifth cycle.

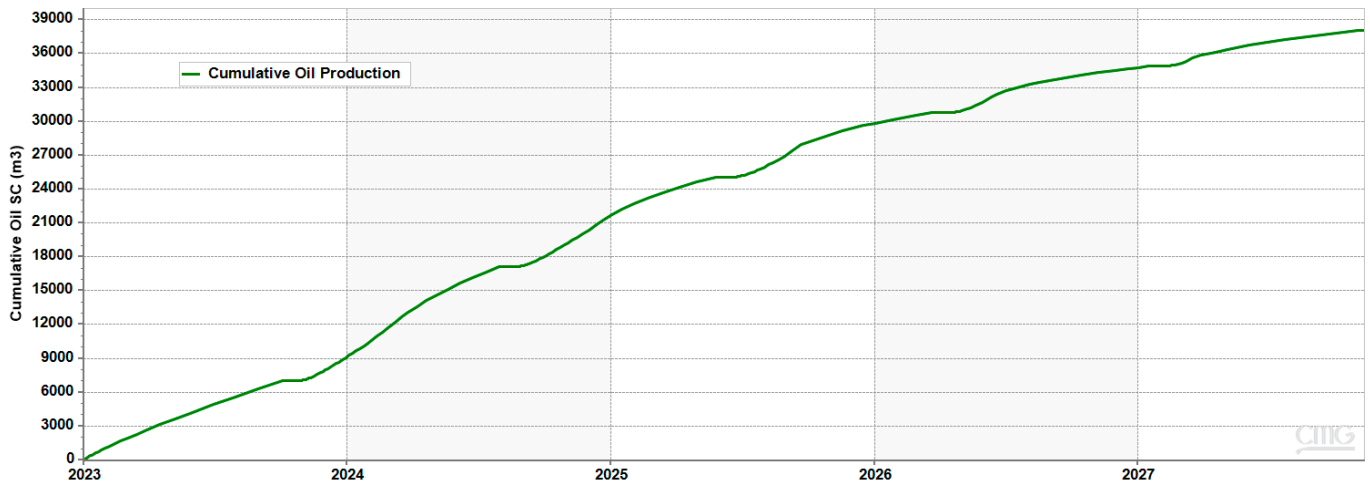


Figure 7. Cumulative oil production of the basic cyclic steam stimulation process with subcritical steam.

Figure 8 shows the comparison of oil production rates and water production rates of the basic cyclic steam stimulation process using subcritical steam with such process using supercritical multi-source and multi-component steam. We further show the cumulative oil recovery curves of the subcritical and supercritical multi-source and multi-component steam injection processes in Figure 9. Figure 10 also shows the solid Dissolvable Rock component distribution (left) and effective porosity (right) distribution of the cyclic steam stimulation process with supercritical multi-source and multi-component steam at the end of the steam injection period of the fifth cycle inside the cross-sectional reservoir. As we can see, the near well region porosity and permeability have been enhanced greatly due to the mineral dissolution effect. The near well region permeability affects the well productivity to a large extent. This provides great potential for oil production

improvements. Figure 11 shows the reservoir temperature (left) and oil saturation (right) distribution of the cyclic steam stimulation process with supercritical multi-source and multi-component steam at the end of the injection period of the fifth cycle. Figure 12 further shows the cross-sectional reservoir temperature (left) and oil saturation (right) distribution of the cyclic steam stimulation process with supercritical multi-source and multi-component steam at the end of the injection period of the fifth cycle. We observed a larger steam chamber and higher steam temperature for supercritical multi-source and multi-component steam injection than the previous process with subcritical steam, which is shown in Figures 5 and 6. Figure 13 shows the cross-sectional reservoir Light Oil's mole fraction in the oil phase distribution (left) and along the horizontal well reservoir Light Oil's mole fraction in the oil phase distribution (right) of the cyclic steam stimulation process with supercritical multi-source and multi-component steam injection at the end of the injection period of the first cycle. Figure 14 further shows the cross-sectional reservoir oil viscosity distribution (left) and along the horizontal well reservoir oil viscosity distribution (right) of the cyclic steam stimulation process with supercritical multi-source and multi-component steam injection at the end of the injection period of the first cycle. Initially, there are no light oil components present inside the reservoir. The near-well Light Oil component distribution is solely due to the pyrolysis reaction of the crude oil. We have observed clear in-situ upgrading of the crude oil in the near-well high-temperature region. In the production period following this upgrade, oil will be produced initially with high productivity, which accounts for part of the improved oil recovery effects. Figure 15 shows the cumulative production of the light oil component and heavy oil component of the cyclic steam stimulation process with supercritical multi-source and multi-component steam injection. As we can see, the light oil component production accounts for approximately 15,000 m³ of crude oil, while the heavy oil component production accounts for about 90,000 m³ of crude oil. The in situ upgrading effect is clearly present in such a process.

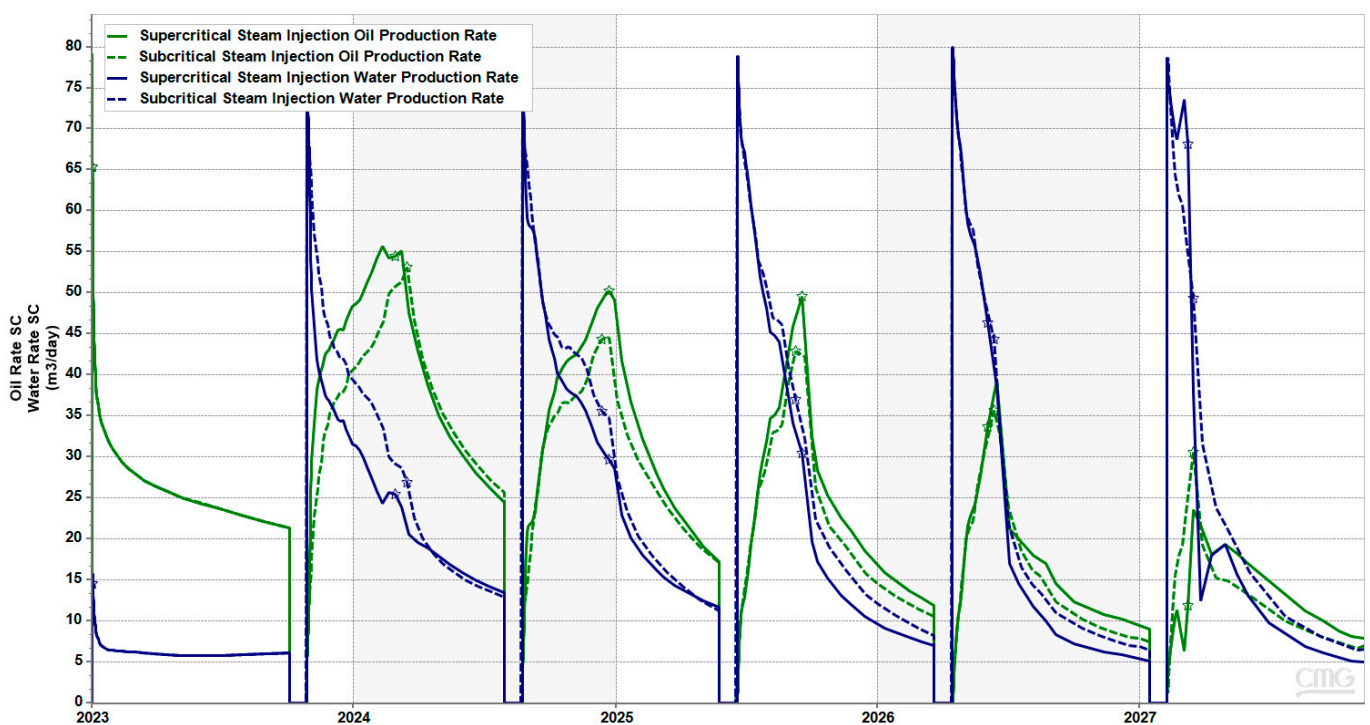


Figure 8. Comparison of oil production rates and water production rates of the basic cyclic steam stimulation process using subcritical steam with such process using supercritical multi-source and multi-component steam.

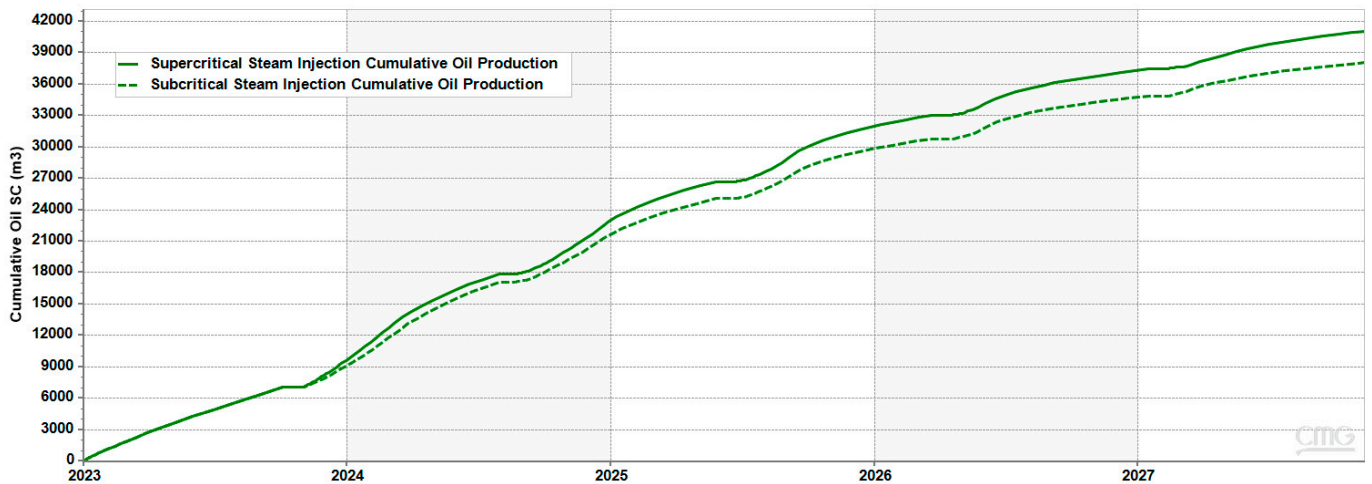


Figure 9. Comparison of cumulative oil production of the basic cyclic steam stimulation process using subcritical steam with such process using supercritical multi-source and multi-component steam.

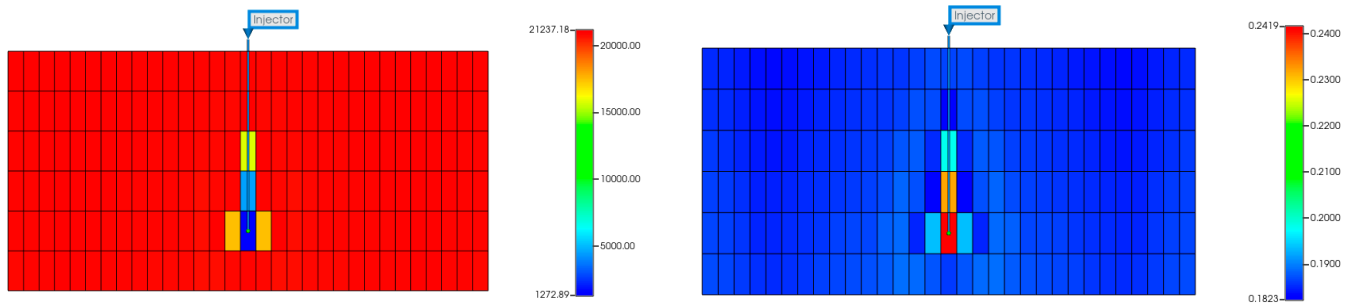


Figure 10. Cross-sectional reservoir solid Dissolvable Rock component distribution (left) and effective porosity (right) distribution of the cyclic steam stimulation process with supercritical multi-source and multi-component steam at the end of the steam injection period of the fifth cycle.

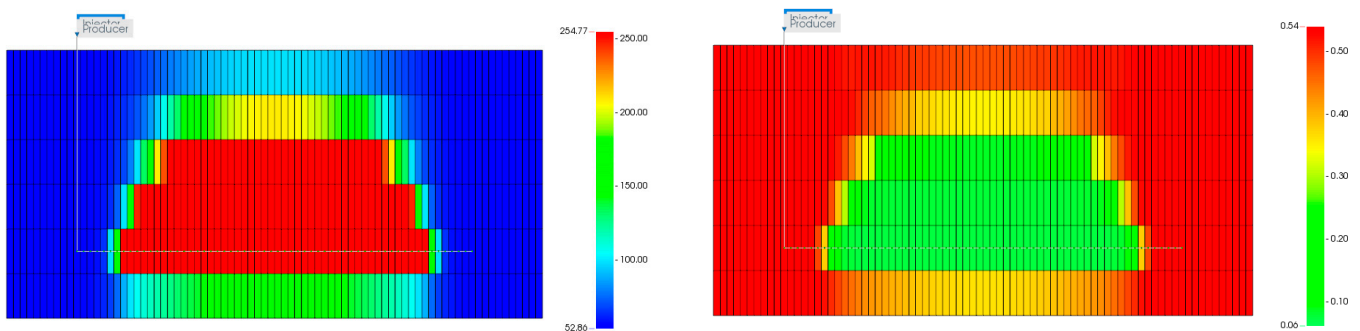


Figure 11. Along the horizontal well, reservoir temperature (left) and oil saturation (right) distribution of the cyclic steam stimulation process with supercritical multi-source and multi-component steam at the end of the injection period of the fifth cycle.

Eventually, we observe incremental oil recovery of about 7.8% when comparing supercritical multi-source and multi-component steam injection to subcritical steam injection. Overall, due to its novel recovery mechanisms of the crude oil pyrolysis reactions, temperature-dependent relative permeability effects, and the mineral dissolution of the rock matrix under high temperature, the supercritical multi-source and multi-component steam injection process has shown clear improvements against the subcritical steam injection process. We are now in the process of further economic evaluations and field pilot designs to deploy such novel technology to one of the horizontal wells in the Lvda-21-2 oil fields. A

field pilot is currently underway, with the supercritical multi-source and multi-component steam generator specially designed for limited space on offshore platforms currently under construction. Reports on improved oil recovery in actual field pilot operations will be discussed in detail in further publications on this topic.

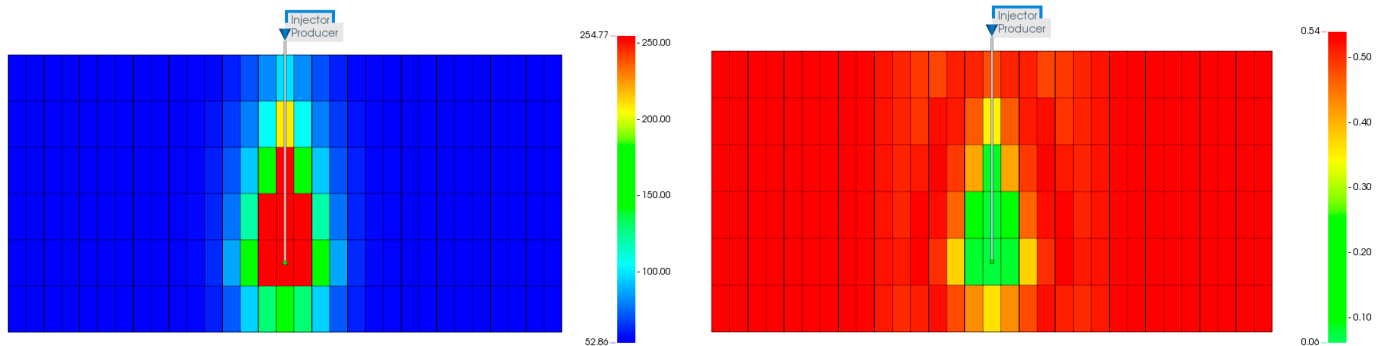


Figure 12. Cross-sectional reservoir temperature (left) and oil saturation (right) distribution of the cyclic steam stimulation process with supercritical multi-source and multi-component steam at the end of the injection period of the fifth cycle.

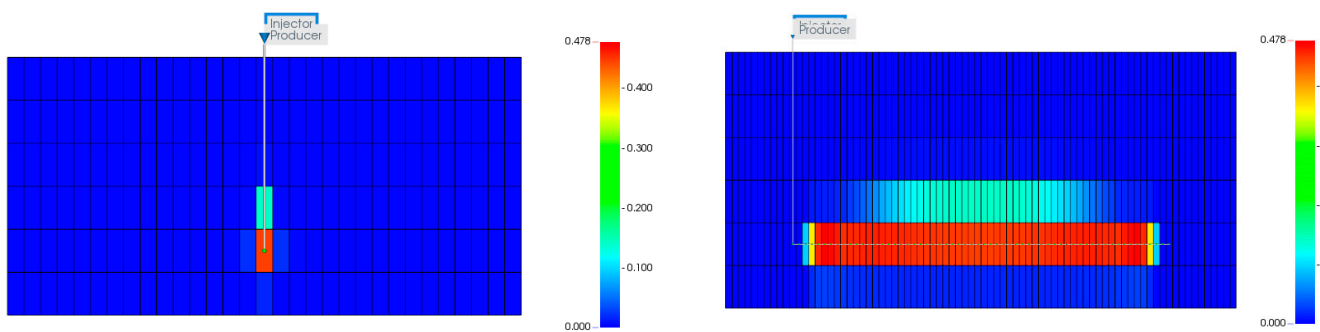


Figure 13. Cross-sectional reservoir light oil's mole fraction in the oil phase distribution (left) and along the horizontal well reservoir light oil's mole fraction in the oil phase distribution (right) of the cyclic steam stimulation process with supercritical multi-source and multi-component steam injection at the end of the injection period of the first cycle.

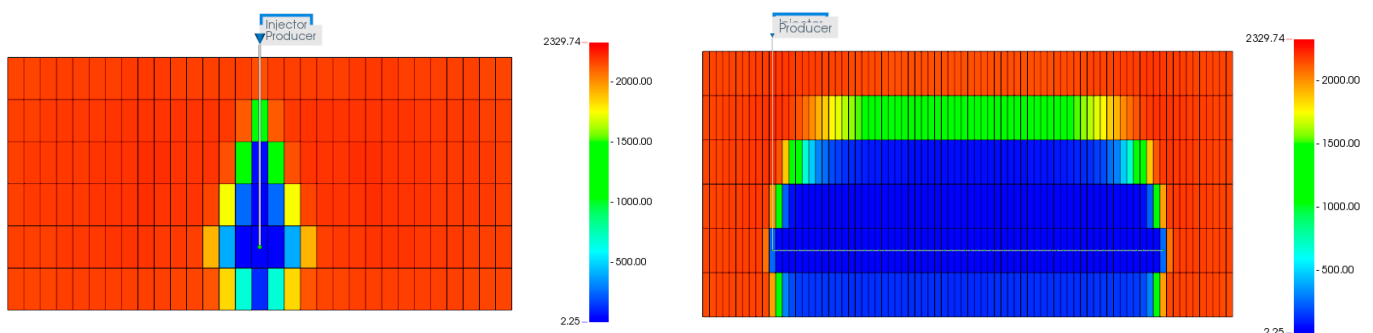


Figure 14. Cross-sectional reservoir oil viscosity distribution (left) and along the horizontal well reservoir oil viscosity distribution (right) of the cyclic steam stimulation process with supercritical multi-source and multi-component steam injection at the end of the injection period of the first cycle.

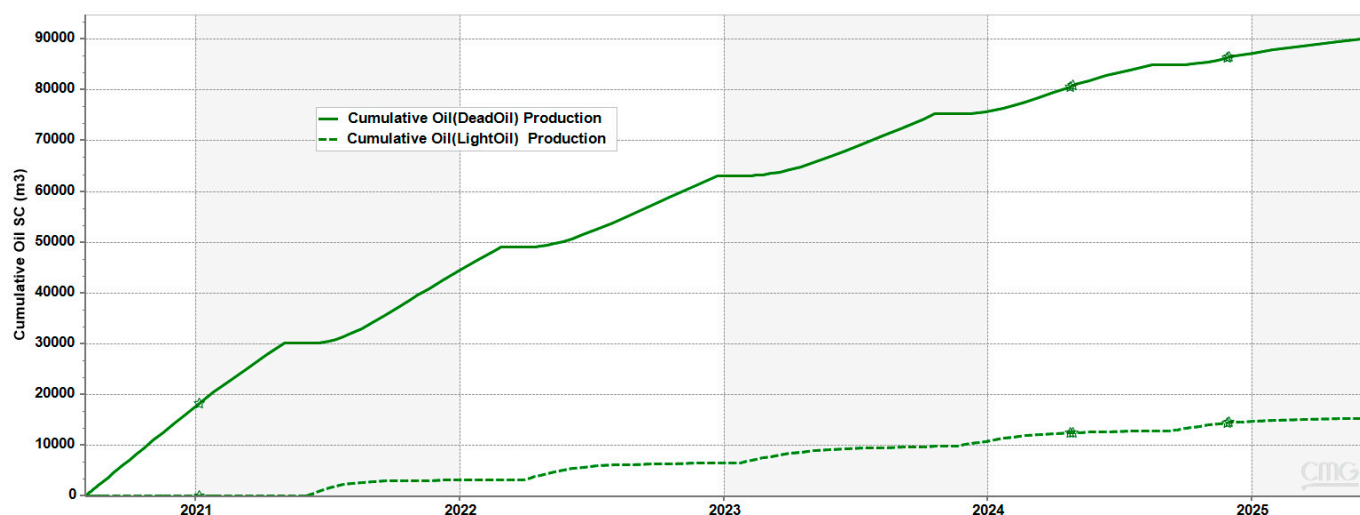


Figure 15. Cumulative production of the light oil component and the heavy oil component of the cyclic steam stimulation process with supercritical multi-source and multi-component steam injection.

4. Discussion

In order to model the novel heavy oil EOR process of supercritical multi-source and multi-component steam injection, we have implemented the default steam thermal properties in CMG STARS. We have also included the pyrolysis chemical reactions by defining a cracking reaction of the Heavy Oil components, which turn into the Light Oil and solid Coke components. The kinetic parameters of this reaction are calibrated according to our in-house laboratory experiment measurements. The temperature-dependent relative permeability is also implemented using the temperature-dependent end point shifts of the water-oil relative permeability curve in CMG STARS. This yields a more water-wet matrix rock under high temperatures. A kinetic chemical reaction, which turns the initially present solid Dissolvable Rock into water under high temperature, is also included to mimic the process of partially dissolving the sandstone rock to enhance the matrix porosity. The Carmen-Kozeny correlation is defined to enhance the effective permeability of the rock as a function of the porosity. These simulation parameters are calibrated according to the laboratory experiments on these complex phenomena. Finally, we observe incremental oil recovery of about 7.8% when comparing supercritical multi-source and multi-component steam injection to subcritical steam injection in our simulations. We are now in the stage of economics evaluations and field pilot designs in deploying such novel technology to the horizontal wells in the Lvda-21-2 oil fields.

5. Conclusions

In this work, we demonstrate the workflow for numerical reservoir simulation of the supercritical multi-source and multi-component steam injection process. We have implemented the thermal properties of supercritical multi-source and multi-component steam, the pyrolysis chemical reactions, the temperature-dependent relative permeability, and the process of partial dissolution of the sandstone rock to enhance the reservoir permeability in a commercial reservoir simulator. Simulations are conducted on the type pattern reservoir model, which represents the Lvda-21-2 heavy oil field in CNOOC's Bohai Bay oil field. Simulation results have shown clear improvements in injecting supercritical multi-source and multi-component steam in cumulative oil recovery when compared to normal steam process using subcritical steam. This serves as a workflow for implementing a numerical simulation of the novel supercritical multi-source and multi-component steam injection recovery process.

Author Contributions: Conceptualization, Q.F. and Z.Z.; methodology, Q.F.; software, Z.Z.; validation, Q.F., J.L. and H.J.; formal analysis, S.W.; investigation, Y.L.; resources, H.W.; data curation, Z.Z.; writing—original draft preparation, Z.Z.; writing—review and editing, Q.F.; visualization, J.L.; supervision, Q.F.; project administration, H.J.; funding acquisition, Q.F. All authors have read and agreed to the published version of the manuscript.

Funding: This work was supported by the CNOOC project “Research on Key Technologies for Offshore Supercritical Multi-source and Multi-component Thermal Fluid Thermal Recovery” (KJGG2022-0605). This work was also supported by the CNOOC project “Research on Key Technologies and Methods for Adaptability and Productivity Prediction of Supercritical Multi-source and Multi-component Thermal Fluid Thermal Recovery” (KJGG2022-0605). This work was also supported by the CNOOC project “Research on the Prediction Method and Numerical Simulation Method for Thermal Recovery Productivity of Supercritical Multi-source and Multi-component Thermal Fluid”.

Data Availability Statement: The data used to support the findings of this study are available from the corresponding author upon request.

Acknowledgments: We appreciate State Key Laboratory of Natural Gas Hydrates, CNOOC Research Institute Ltd. for permission to publish this work.

Conflicts of Interest: Authors Qiang Fu, Hongmei Jiao, Huiyun Wen, Yongfei Liu were employed by the CNOOC Research Institute Ltd. The authors declare that this study received funding from CNOOC Research Institute Ltd. The funder was not involved in the study design, collection, analysis, interpretation of data, the writing of this article or the decision to submit it for publication.

References

1. Prats, M. *Thermal Recovery*; Society of Petroleum Engineers: Richardson, TX, USA, 1982; ISBN 978-1-61399-548-8.
2. Couderc, B.M.; Verpeaux, J.F.; Monfrin, D.; Quettler, L.H. Emeraude Vapeur: A Steam Pilot in an Offshore Environment. *J. Pet. Sci. Eng.* **1989**, *2*, 179–191. [\[CrossRef\]](#)
3. Sun, Y.; Zhao, L.; Lin, T.; Liu, H.; Sun, Y.; Zhong, L.; Dong, Z.; Hou, J.; Li, Y. Case Study: Thermal Enhance Bohai Offshore Heavy Oil Recovery by Co-stimulation of Steam and Gases. In Proceedings of the SPE Heavy Oil Conference, Calgary, AB, Canada, 11–13 June 2013. [\[CrossRef\]](#)
4. Liu, Y.; Han, X.; Zou, J.; Wang, Q.; Wang, H.; Liu, H.; Jiang, Z. New Progress of the Offshore Thermal Recovery Technologies in Bohai Bay, China. In Proceedings of the SPE/IATMI Asia Pacific Oil & Gas Conference and Exhibition, Jakarta, Indonesia, 17–19 October 2017. [\[CrossRef\]](#)
5. Dong, X.; Liu, H.; Hou, J.; Zhang, T.; Zhan, J.; Chen, Z.; Hong, C. The Thermal Recovery Methods and Technical Limits of Bohai Offshore Heavy Oil Reservoirs: A Case Study. In Proceedings of the Offshore Technology Conference Brasil, Rio de Janeiro, Brazil, 27–29 October 2015. [\[CrossRef\]](#)
6. Liu, Y.; Zou, J.; Meng, X.; Zhong, L.; Wang, Q.; Zhang, W.; Zhou, F.; Han, X. Progress in Bohai Offshore Heavy Oil Thermal Recovery. In Proceedings of the Offshore Technology Conference Asia, Kuala Lumpur, Malaysia, 22–25 March 2016. [\[CrossRef\]](#)
7. Han, X.; Zhong, L.; Tang, X.; Wang, H.; Zou, J.; Wang, Q.; Liu, H. Ten-Year Pilot Test of Steam and Flue Gas Stimulation for Offshore Heavy Oilfield. In Proceedings of the Offshore Technology Conference Asia, Virtual, 2–6 November 2020. [\[CrossRef\]](#)
8. Wu, J.; Lin, H.; Huang, Y.; Wang, H.; Zhou, S.; Fu, Q. Hydrocyclone Micrometer Sized Separation Technology for Exploitation of Natural Gas Hydrate. In Proceedings of the Offshore Technology Conference, Houston, TX, USA, 4–7 May 2020. [\[CrossRef\]](#)
9. Chen, M.; Li, Q.; Zhou, S.; Pang, W.; Lyu, X.; Zhu, J.; Fu, Q.; Lyu, C.; Ge, Y. Dynamic Characterization of Pore Structures in Hydrate-Bearing Sediments During Hydrate Phase Transition. In Proceedings of the SPE Annual Technical Conference and Exhibition, San Antonio, TX, USA, 16–18 October 2023. [\[CrossRef\]](#)
10. Wang, S.; Zhang, F.; Liu, D.; Zhu, Q.; Ge, T.T. Physical—Numerical Simulation Integration of Super—Critical Steam—Flooding in Offshore Extra—Heavy Oil Reservoir. *Spec. Oil Gas Reserv.* **2020**, *27*, 138–144.
11. Hascakir, B.; Kovscek, A.R. Reservoir Simulation of Cyclic Steam Injection Including the Effects of Temperature Induced Wettability Alteration. In Proceedings of the SPE Western Regional Meeting, Anaheim, CA, USA, 27–29 May 2010. [\[CrossRef\]](#)
12. STARS 2019. *STARS Version 2019 User’s Guide*; Computer Modeling Group Ltd.: Calgary, AB, Canada, 2019.
13. Ursenbach, M.G.; Moore, R.G.; Bennion, D.W.; Belgrave, J. Laboratory Situ Combustion Behavior of Athabasca Oil Sands. In Proceedings of the Technical Meeting/Petroleum Conference of The South Saskatchewan Section, Regina, SK, Canada, 17–19 October 1993. [\[CrossRef\]](#)

14. Hayashitani, M.; Bennion, D.W.; Donnelly, J.K.; Moore, R.G. Thermal Cracking Models for Athabasca Oil Sands Oil. In Proceedings of the SPE Annual Fall Technical Conference and Exhibition, Houston, TX, USA, 1–3 October 1978. [[CrossRef](#)]
15. Hascakir, B.; Ross, C.M.; Castanier, L.M.; Kavscek, A.R. Fuel Formation During In-Situ Combustion of Heavy Oil. In Proceedings of the SPE Annual Technical Conference and Exhibition, Denver, Colorado, USA, 30 October–2 November 2011. [[CrossRef](#)]

Disclaimer/Publisher’s Note: The statements, opinions and data contained in all publications are solely those of the individual author(s) and contributor(s) and not of MDPI and/or the editor(s). MDPI and/or the editor(s) disclaim responsibility for any injury to people or property resulting from any ideas, methods, instructions or products referred to in the content.